Trypanothione reductase inhibition and anti-leishmanial activity of all-hydrocarbon stapled α-helical peptides with improved proteolytic stability

Marta Ruiz-Santaquiteria,[a] Sonia de Castro,[a] Miguel A. Toro,[b] Héctor de Lucio,[b] Kilian Jesús Gutiérrez,[b] Pedro A. Sánchez-Murcia,[c] María Ángeles Jiménez,[d] Federico Gago,[c] Antonio Jiménez-Ruiz,[b] María-José Camarasa,[a] and Sonsoles Velázquez[a]*

[a] *Instituto de Química Médica (IQM-CSIC), E-28006 Madrid, Spain*

[b] *Departamento de Biología de Sistemas, Universidad de Alcalá, E-28805 Alcalá de Henares, Madrid, Spain*

[c] *Área de Farmacología, Departamento de Ciencias Biomédicas, Unidad Asociada al IQM-CSIC, Universidad de Alcalá, E-28805 Alcalá de Henares, Madrid, Spain*

[d] *Instituto Química-Física Rocasolano (IQFR-CSIC), Madrid, Spain*

Abbreviations- CD, circular dichroism; CPP, cell-penetrating peptide; ELISA, Enzyme-Linked ImmunoSorbent Assay; FCS, fetal calf serum; FITC fluorescein isothiocyanate; H-GR, human glutathione reductase; HCTU, *O*-(6-chlorobenzotriazol-1-yl)-*1,1,3,3-*tetramethyluronium hexafluorophosphate, IC_{50}, inhibitory concentration 50; Li-TryR, *Leishmania infantum* trypanothione reductase; EC_{50}, effective concentration 50; MD, molecular dynamics; PEG, polyethylene glycol; PPIs, protein-protein interaction inhibitors; PI, propidium iodide; RCM, ring-closing metathesis; SPPS, solid phase peptide synthesis, TFE, trifluorethanol; VL, visceral leishmaniasis.

* Corresponding author: Dr. Sonsoles Velázquez
Instituto de Química Médica (CSIC), C/ Juan de la Cierva 3
E-28006 Madrid (Spain) Phone number: (+34) 912587458
e-mail: iqmsv29@iqm.csic.es

Abstract—Trypanothione reductase (TryR) is a well-established target in the search for novel antitrypanosomal and antileishmanial agents. We have previously identified linear and lactam-bridged 13-residue peptides derived from an α-helical region making up part of the dimeric interface of *Leishmania infantum* TryR (Li-TryR) which prevent trypanothione reduction by disrupting enzyme dimerization. We now show that *i,i+4* side-chain cross-linking with an all-hydrocarbon staple stabilizes the helical structure of these peptides and significantly improves their resistance to protease cleavage relative to previous linear and cyclic lactam analogues. Interestingly, replacement of the amide bridge by the hydrocarbon staple at the same cyclization positions generates derivatives (**2** and **3**) that similarly inhibit oxidoreductase activity of the enzyme but unexpectedly stabilize the TryR homodimer. The most proteolytically stable peptide **2** covalently linked to oligoarginines displayed potent *in vitro* leishmanicidal activity against *L. infantum* parasites.

Graphical abstract
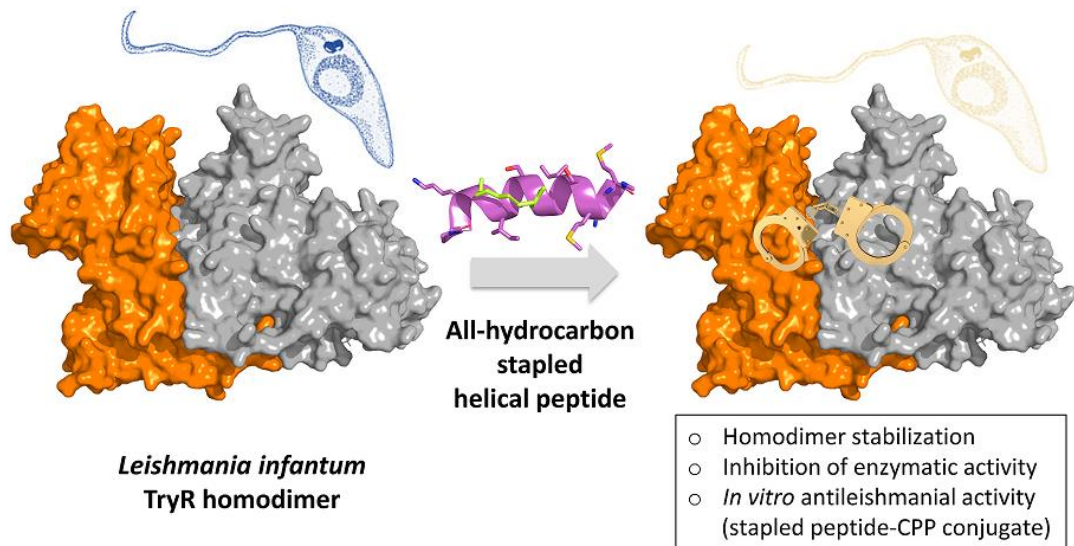
Highlights

- All-hydrocarbon stapled peptides were derived from the monomer-monomer interface of Li-TryR

- Li-TryR oxidoreductase activity was potently inhibited by these peptides

- Unexpected stabilization of the TryR homodimer was observed

- α-helicity and proteolytic stability were significantly increased relative to their linear counterparts

- Conjugation with cell-penetrating peptides resulted in leishmanicidal activity

Introduction

Leishmania parasites are the causative agents of leishmaniasis, a neglected tropical disease that is still endemic in more than 80 countries worldwide, according to the World Health Organization. The most lethal form of the disease is visceral leishmaniasis (VL), also known as kala-azar, predominantly caused by *Leishmania donovani* and *Leishmania infantum* species which is invariably fatal if left untreated [1]. Because resistance to current therapeutic options, which involve long and costly treatments, is commonplace and the medicines used are considerably toxic [2-4], there is a pressing need for innovative drugs that act on new molecular targets and/or employ novel mechanisms of action.

A frequently exploited strategy to develop potent and specific antileishmanial drugs is to try and disrupt a metabolic pathway that is vital for the parasite and has no direct counterpart in the host. Trypanothione reductase (TryR), due to its key role in the maintenance of cellular redox homeostasis in *Leishmania* and other trypanosomatids, is an essential enzyme for survival of these parasites [5,6]. The Try/TryR system is analogous to the mammalian glutathione/glutathione reductase (GSH/GR) pair involved in redox status regulation. However, the significant differences in the active site architectures of the enzymes from parasites and human beings facilitate the development of inhibitors selective for TryR over H-GR. TryR is a well-established drug target for antiparasitic drug design, with almost all known inhibitors targeting its active site [7-9]. This enzyme belongs to the large and well-characterized family of FAD-dependent NADPH oxidoreductases. From a structural viewpoint, TryR is a homodimer containing distinct domains for FAD-binding, NADPH-binding and interfacial recognition.

We recently explored an alternative approach for TryR inhibition that consists of disrupting protein-protein interactions (PPIs) at the homodimer interface [10]. Computational and experimental site-directed mutagenesis studies identified and validated E436 as a key amino acid ("hot spot") for the structural stability and function of the *Leishmania infantum* TryR (Li-

TryR) homodimer. The "proof of concept" was obtained when a small library of linear peptides representing rational variations of the α-helix spanning residues P435 to M447 was designed and tested. All of these peptides contained a Glu residue at position 2 (Glu^2) equivalent to the crucial E436 of Li-TryR. Unexpectedly, the linear PKIIQSVGIS-Nle-K-Nle 13-residue peptide **1**, containing Lys^2 in place of Glu^2, outperformed all other peptides in inhibiting both Li-TryR dimerization and oxidoreductase activity [10]. A rationale for these findings was provided by results from molecular dynamics (MD) simulations, which showed Lys^2 of the peptide can establish a strong electrostatic interaction with both D432 and E436 in the Li-TryR monomer it putatively binds to. Nonetheless, these peptide prototypes, despite their potency in inhibiting TryR dimerization and enzymatic activity *in vitro*, were ineffective against *L. infantum* axenic amastigotes and promastigotes, most likely due to their inability to cross the cell membrane, as assessed by using FITC-labeled peptides [10].

Short peptide sequences normally have negligible or random structure in water, whereas their binding targets usually recognize a specific conformation. The biological activity of peptide analogs can be improved by stabilizing their secondary structure and limiting their proteolysis through covalent cyclization [11-13], most often by means of side chain-to-side chain linkage. In stabilizing α-helices, the use of lactam bridges [14-16] and, more recently, short hydrocarbon chains [17-19] as staples has proven to be a successful approach to enhance helicity and to limit degradation by proteases of the resulting stapled peptides. In the case of hydrocarbon linkages, improvements in oral absorption [20] and cell permeability [21-23] have also been reported although these are two of the most significant yet poorly understood aspects of peptide stapling technology [24,25]. So far, numerous examples of conformationally restricted peptides for several therapeutic targets have been reported to succesfully modulate PPIs [26-28].

We recently reported [29] an example of helical content stabilization by preparing and testing a series of cyclic analogues of the most potent linear prototype TryR inhibitor **1** that were amide-bridged between amino acid side chains *i* and *i+4*. Our results indicated that several cyclic analogues retained potent inhibitory activity against the enzyme (when the staple was properly located) but also that their proteolytic stability against proteinase K was only modestly increased in comparison to those of their linear counterparts. Interestingly, we later demonstrated, for the first time to the best of our knowledge, *in vitro* activity against *Leishmania infantum* of peptide-based inhibitors of TryR dimerization when they were conjugated to cationic cell-penetrating peptides (CPPs) [29].

We herein report the synthesis of all-hydrocarbon stapled peptides **2** and **3** (Figure 1), derived from the most potent linear prototype **1**, which were designed as inhibitors of Li-TryR dimerization and activity with improved proteolytic stability over those of previous linear and lactam-bridged peptides. Their potential to penetrate cells and exert their leishmanicidal effects was also evaluated *in vitro*. Hydrocarbon cross-links were introduced between amino acid side-chains that are separated by one helical turn (*i, i+4*). The location of the hydrocarbon bridge at the non-recognition side was chosen on the basis of results obtained for the first series of lactam-bridged analogues, for which the best activities were found upon cyclization between positions 3/7 and 4/8 of the peptide sequence. Other possible cyclization positions resulted in a significant potency loss [29]. Thus, in line with these precedents, stapling positions 3/7 and 4/8, leading to hydrocarbon-stapled peptides **2** and **3**, respectively, were selected. Fluorescein–labeled peptide conjugate **4** and the most proteolytically stable hydrocarbon-stapled peptide conjugated to a polyarginine CPP (**5**) (Figure 1) were also prepared for cellular uptake studies using fluorescence microscopy and *in vitro* evaluation of their antileishmanial activity.
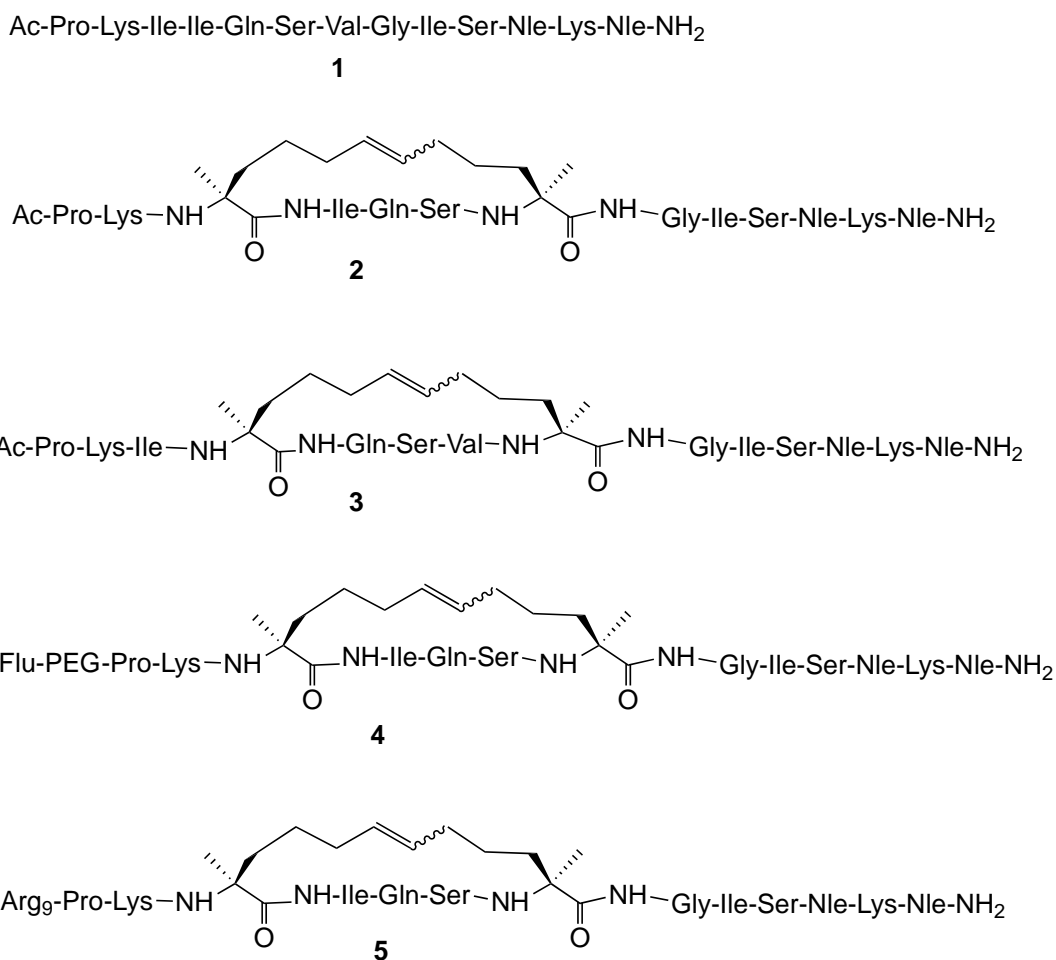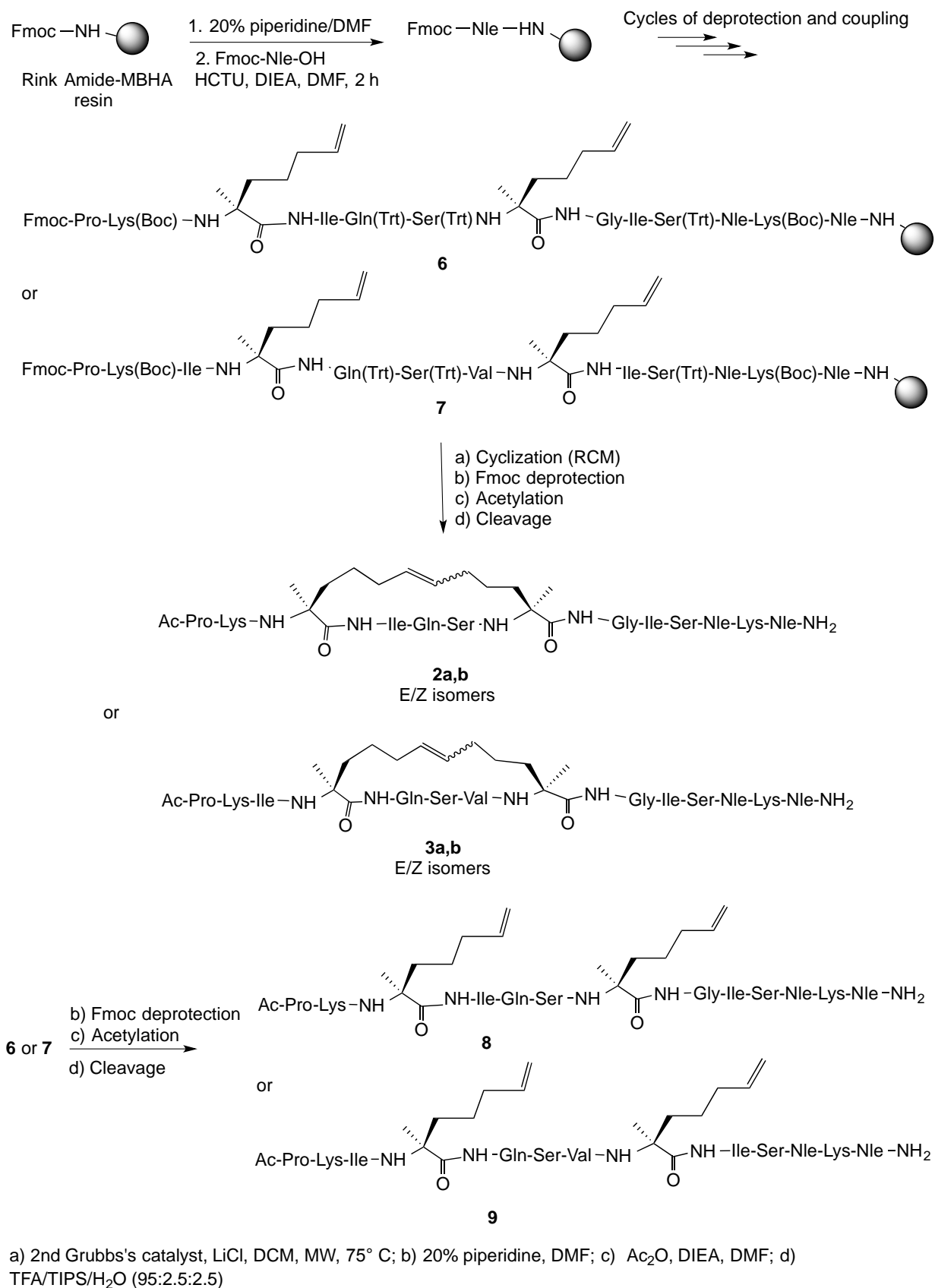
Ac-Pro-Lys-Ile-Ile-Gln-Ser-Val-Gly-Ile-Ser-Nle-Lys-Nle-NH$_2$

1

Ac-Pro-Lys—NH〜C(O)—NH-Ile-Gln-Ser—NH〜C(O)—NH—Gly-Ile-Ser-Nle-Lys-Nle-NH$_2$

2

Ac-Pro-Lys-Ile—NH〜C(O)—NH-Gln-Ser-Val—NH〜C(O)—NH—Gly-Ile-Ser-Nle-Lys-Nle-NH$_2$

3

Flu-PEG-Pro-Lys—NH〜C(O)—NH-Ile-Gln-Ser—NH〜C(O)—NH—Gly-Ile-Ser-Nle-Lys-Nle-NH$_2$

4

Arg$_9$-Pro-Lys—NH〜C(O)—NH-Ile-Gln-Ser—NH〜C(O)—NH—Gly-Ile-Ser-Nle-Lys-Nle-NH$_2$

5

Figure 1. Structures of the linear prototype **1** and the designed all-hydrocarbon stapled compounds **2-5** synthesized in this work.

Results and Discussion

Chemical synthesis

The synthesis of the all-hydrocarbon stapled peptides was performed manually following standard solid-phase peptide synthesis (SPPS) protocols using a Rink amide MBHA polystyrene resin and N-Fmoc/^{t}Bu chemistry. The peptides were isolated acetylated at the N-terminus and as carboxamides at the C-terminal end. A low load resin (0.38 mmol/g) was used to minimize oligomer formation during the side-chain to side-chain cyclization.

The preparation of hydrocarbon-stapled peptides **2** and **3** was carried out by introduction of two units of Fmoc-(*S*)-α-methyl-α-pentenylglycine at the suitable positions of the sequence in the elongation step as previously described by Verdine and co-workers (Scheme 1) [30,31]. Linear precursors **8** and **9** were prepared from the corresponding solid-supported linear peptides **6** and **7** after Fmoc-deprotection, acetylation and final cleavage from the resin. Dicarba bridge formation was accomplished through on-resin ring-closing metathesis (RCM) using Grubb's second-generation ruthenium catalyst. Initial efforts to perform RCM at room temperature or prolonged heating at 90 °C for 12 h in a pressure tube using CH_2Cl_2 as the solvent resulted in little to no conversion to the stapled peptide. However, when the mixture was heated under MW irradiation at 75 °C for 1 h, complete conversion was detected by HPLC-MS after cleavage of a small quantity of peptidyl-resin [32]. Next, the *N*-terminus of the peptides was acetylated, cleaved from the resin under standard conditions and purified by semi-preparative HPLC. Both *E* and *Z* isomers of **2** and **3** were detected by HPLC, which allowed the separation, isolation and subsequent biological evaluation of **2a** and **2b**. In the case of stapled peptide **3a** only the major isomer could be isolated. *E* and *Z* isomers are generally distinguished by the value of the $^3J_{HH}$ coupling constant between the vinyl protons (Hε and Hε' in the case of peptides **2a,b** and **3a**). This $^3J_{HH}$ constant could not be measured in either isomer **2a** or **2b** because both isomers have similar ^1H chemical shifts for Hε and Hε' protons (5.47 ppm in major isomer **2a**, and 5.36 ppm in minor isomer **2b**; Tables S1-S2). In the case of the major isomer of **3**, the ^1H chemical shifts for the protons Hε and Hε' are distinguishable, and the $^3J_{HH}$ coupling constant between them is approximately 18.6-19.0 Hz, which indicates that, most likely, it corresponds to the *E* isomer.

Fmoc—NH—⬤

Rink Amide-MBHA resin

1. 20% piperidine/DMF
2. Fmoc-Nle-OH
HCTU, DIEA, DMF, 2 h

Fmoc—Nle—HN—⬤

Cycles of deprotection and coupling

Fmoc-Pro-Lys(Boc)—NH— —NH-Ile-Gln(Trt)-Ser(Trt) NH— —NH~Gly-Ile-Ser(Trt)-Nle-Lys(Boc)-Nle—NH—⬤

6

or

Fmoc-Pro-Lys(Boc)-Ile—NH— —NH·Gln(Trt)-Ser(Trt)-Val—NH— —NH~Ile-Ser(Trt)-Nle-Lys(Boc)-Nle—NH—⬤

7

a) Cyclization (RCM)
b) Fmoc deprotection
c) Acetylation
d) Cleavage

Ac-Pro-Lys—NH— —NH—Ile-Gln-Ser·NH— —NH~Gly-Ile-Ser-Nle-Lys-Nle-NH$_2$

2a,b
E/Z isomers

or

Ac-Pro-Lys-Ile—NH— —NH-Gln-Ser-Val—NH— —NH~Gly-Ile-Ser-Nle-Lys-Nle-NH$_2$

3a,b
E/Z isomers

6 or 7

b) Fmoc deprotection
c) Acetylation
d) Cleavage

Ac-Pro-Lys—NH— —NH-Ile-Gln-Ser—NH— —NH~Gly-Ile-Ser-Nle-Lys-Nle—NH$_2$

8

or

Ac-Pro-Lys-Ile—NH— —NH-Gln-Ser-Val—NH— —NH~Ile-Ser-Nle-Lys-Nle—NH$_2$

9

a) 2nd Grubbs's catalyst, LiCl, DCM, MW, 75° C; b) 20% piperidine, DMF; c) Ac$_2$O, DIEA, DMF; d) TFA/TIPS/H$_2$O (95:2.5:2.5)
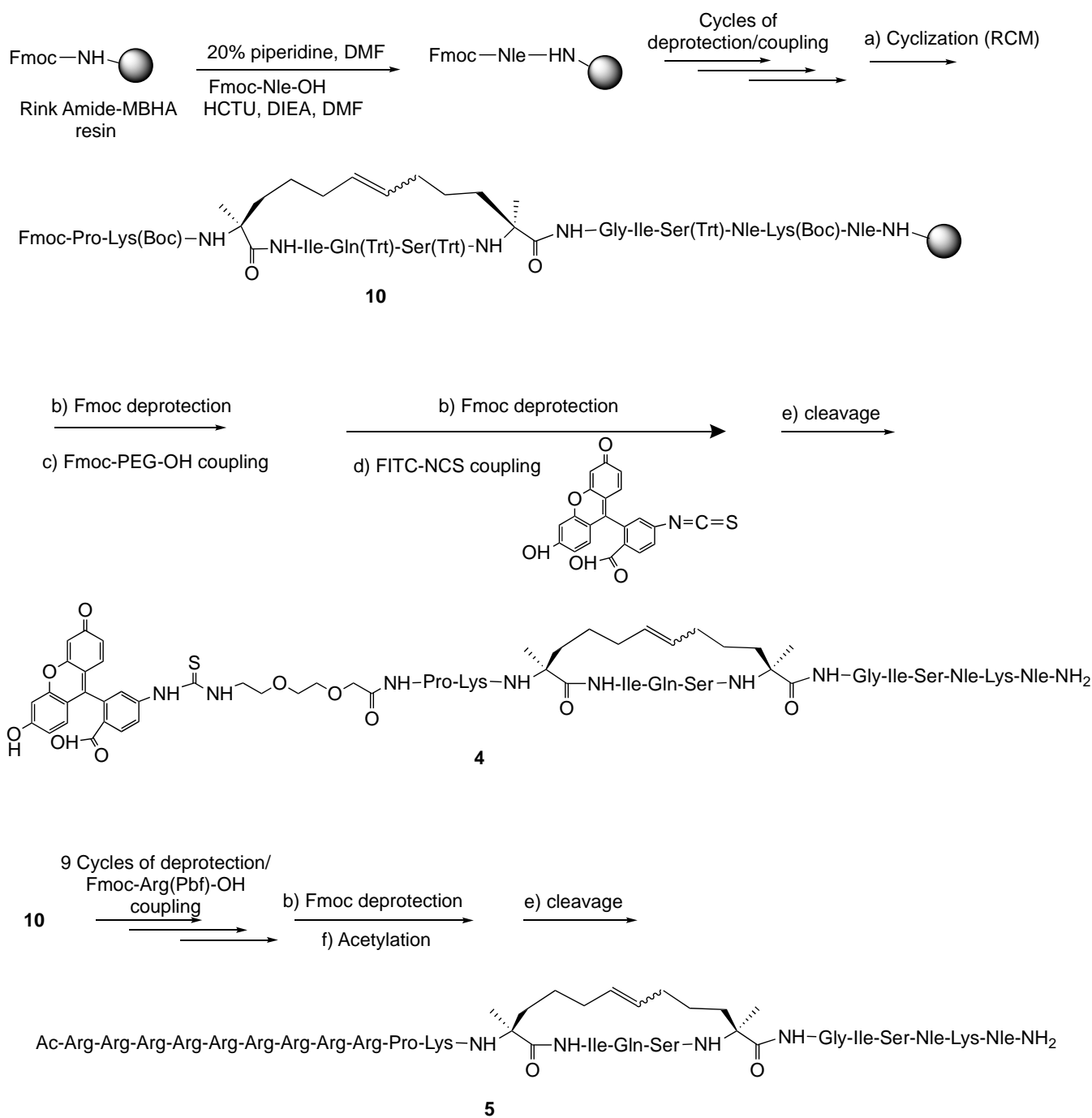
Scheme 1. Synthesis of all-hydrocarbon stapled peptides **2** and **3** and the linear precursors **8** and **9**.

Fluorescein–labeling of the most proteolytically stable **2a** was achieved by linking the *N*-terminal group to FITC through a PEG linker (to increase aqueous solubility). To this end, standard sequences of Fmoc-deprotection and coupling with Fmoc-PEG-OH and FITC-NCS followed by TFA cleavage from the resin gave the desired compound **4 (**Scheme 2).

Finally, to deliver the peptides into the parasites for leishmanicidal *in vitro* evaluation, the *N*-terminal end of **2a** was covalently linked to a polyarginine (R_9) chain using standard SPPS methodology (compound **5**, Scheme 2), as previously reported for our CPP-conjugates of linear peptide prototypes, lactam-bridged analogues and α,β-peptide foldamers [10,29,33].

All hydrocarbon-stapled peptides and linear precursors in this work were characterized by analytical HPLC and ESI-MS or MALDI-TOF after purification on a Biotage Isolera (linear analogues) or by semi-preparative HPLC (cyclic analogues) leading to the linear and cyclic peptides in low/moderate yields and high purity (>95%).

Fmoc—NH—⬤

Rink Amide-MBHA resin

20% piperidine, DMF

Fmoc-Nle-OH
HCTU, DIEA, DMF

Fmoc—Nle—HN—⬤

Cycles of deprotection/coupling

a) Cyclization (RCM)

Fmoc-Pro-Lys(Boc)—NH—NH-Ile-Gln(Trt)-Ser(Trt)—NH—NH—Gly-Ile-Ser(Trt)-Nle-Lys(Boc)-Nle-NH—⬤

10

b) Fmoc deprotection

c) Fmoc-PEG-OH coupling

b) Fmoc deprotection

d) FITC-NCS coupling

e) cleavage

N=C=S

OH OH

NH—Thiourea—PEG—NH—Pro-Lys—NH—NH-Ile-Gln-Ser—NH—NH—Gly-Ile-Ser-Nle-Lys-Nle-NH₂

4

9 Cycles of deprotection/
Fmoc-Arg(Pbf)-OH
coupling

10

b) Fmoc deprotection

f) Acetylation

e) cleavage

Ac-Arg-Arg-Arg-Arg-Arg-Arg-Arg-Arg-Arg-Pro-Lys—NH—NH-Ile-Gln-Ser—NH—NH—Gly-Ile-Ser-Nle-Lys-Nle-NH₂

5

a) 2nd Grubbs's catalyst, LiCl, DCM, MW, 75° C; b) 20% piperidine, DMF; c) Fmoc-PEG-OH, HCTU, DIEA, DMF; d) FITC-NCS, DIEA, DMF ; e) TFA/TIPS/H₂O (95:2.5:2.5); f) Ac₂O:DIEA:DMF

Scheme 2. Synthesis of the major isomers of fluorescently labeled hydrocarbon-stapled peptide **4** and polyarginine-stapled conjugate **5**.

CD studies and proteolytic stability

We used circular dichroism (CD) to determine the effect of the olefinic cross-link on the helical propensity of the peptides. The CD spectra were acquired in water in the presence of the secondary structure-promoting solvent 2,2,2-trifluoroethanol (TFE) (30% TFE/water) [34,35]. TFE was selected as cosolvent due to the poor solubility of the linear hydrophobic peptide **1** in water. As expected, **2a** and **3a** showed the dual minima at 222 nm and 208 nm typical of α-helices in contrast to the linear prototype **1**, which exhibited a CD spectrum characteristic of an unstructured peptide (Figure 2). The percentage of α-helicity calculated for **2a** and **3a,** as calculated from the molar elipticity value at 222 nm and the number of amino acids using the equation of Baldwin and col. [36], is 64 and 43%, respectively. Similar enhancements of helicity have been reported previously in related lactam-bridged peptide analogues [29].
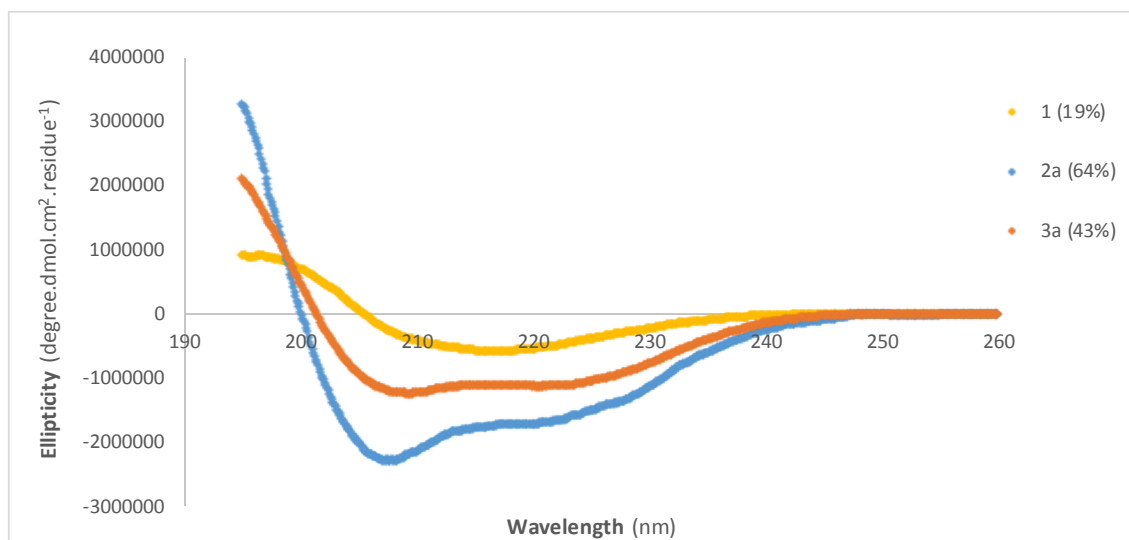

Figure 2. CD spectra and experimentally determined helicities (%) of hydrocarbon-stapled peptides **2a** and **3a** and linear peptide **1.**

We next compared the susceptibilities to degradation by proteinase K, a serine protease with broad substrate specificity, of the linear prototype **1** and the major isomers of hydrocarbon-

stapled peptides **2a** and **3a**. The half-life of both **2a** and **3a** significantly increased (up to 18-fold) compared to those of **1** ($t_{1/2}$ values of 418 and 212 min *vs* 23 min) and the previously described lactam-bridged analogues ($t_{1/2}$ values of 52 and 64 min) [29].

Biological activity

Enzymatic assays

The effect of **2a** and **3a** and their linear precursors **8** and **9** on the activity and dimeric status of Li-TryR was evaluated (Table 1). Our results demonstrate that stapling modestly decreases the potency of the compounds as Li-TryR inhibitors relative to the linear peptide **1** and the corresponding 3,7- or 4,8- lactam-bridged analogues (Table 1). In stark contrast, their activity as disruptors of Li-TryR dimerization is completely abolished and, surprisingly, some of them (analogues **2a**, **3a** and **9**) even behave as stabilizers of the dimeric form of the enzyme, as demonstrated by the increased ELISA signal derived from the Li-TryR dimer after incubation with these compounds (Figure S4). This stabilizing effect had not been previously observed and might be indicative of an unexpected interaction of the stapled peptides with Li-TryR that somehow impairs dimer disruption.

A deleterious effect on the disruptive activity of the peptides upon stapling was previously observed for analogues containing a Glu residue at position 2 (Glu^2) [32]. Thus, the present study reinforces our previous observations about the important nature of the covalent linker (lactam *vs* hydrocarbon) for TryR dimer destabilization and is in line with observations by others suggesting that the increase in overall hydrophobicity of the stapled peptide likely impacts not only the protein structure but also the interdomain water dynamics [37] because the water molecules present at the interface between protomers are likely to behave very differently depending on the polarity of the linker. The intriguing paradox is that inhibition of TryR activity appears to arise from *either* stabilization *or* destabilization of the homodimer. In

both cases, the protein motions that presumably occur during the catalytic cycle are likely to be prevented or hampered due to binding of the peptide to one of the monomers. It is conceivable that the ensuing decrease in reduced trypanothione formation leads to the observed growth inhibition.

Table 1. Potency of hydrocarbon-stapled peptides **2** and **3** and linear precursors **8** and **9** in the Li-TryR oxidoreductase activity and dimerization assays.

Peptide	Activity assay IC_{50} (µM)[a]	Dimerization assay IC_{50} (µM)
1 (linear prototype)	1.2 ± 0.2	13.5 ± 2.4
3,7-lactam-bridged analogue[c]	0.9 ± 0.1	9.9 ± 1.6[b]
4,8-lactam-bridged analogue[c]	5.3 ± 0.8	14.4 ± 1.8[b]
2a (3,7-hydrocarbon-stapled, major isomer)	6.7 ± 0.4	Homodimer stabilizer
2b (3,7-hydrocarbon-stapled, minor isomer)	>25	No effect
3a (4,8-hydrocarbon-stapled, major isomer)	6.4 ± 0.6	Homodimer stabilizer
8 (linear precursor **2)**	28.2 ± 1.7	No effect
9 (linear precursor **3)**	12.5 ± 1.1	Homodimer stabilizer

[a] >25 indicates that the IC_{50} is higher than 25 µM (maximum concentration assayed). Results are representative of three independent experiments each performed in triplicate. [b] Data from lactam-bridged analogues [29] are included for comparative purposes.

Because of the functional and structural similarities between Li-TryR and human GR (H-GR), we compared the activity of peptides **2a** and **3a** against both enzymes under similar conditions. Surprisingly, both Li-TryR inhibitors activate, rather than inhibit, H-GR's oxidoreductase activity (Figure 3).
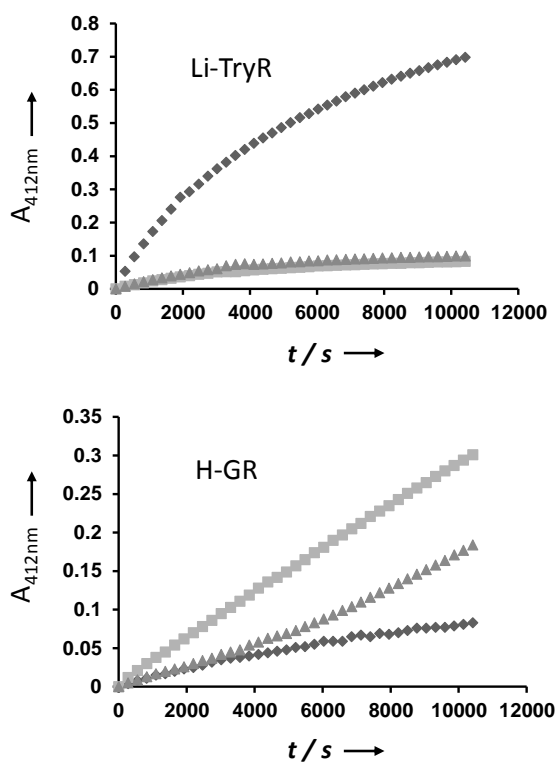
Figure 3. Oxidoreductase activity of Li-TryR and H-GR measured as the increase in absorbance at 412 nm (reduction of DTNB coupled to $T[SH]_2$ or GSH production, respectively). Activity of the enzymes in the presence of either 1.75% DMSO (♦), 75 μM **2a** (■) or 75 μM **3a** (▲).

In vitro antileishmanial activity

The all-hydrocarbon stapled analogues **2a** and **3a** and the linear precursors **8** and **9** were tested *in vitro* against *L. infantum* promastigotes and axenic amastigotes to evaluate their antileishmanial activity. Edelfosine and miltefosine were included in the assays as positive controls. None of the compounds displayed any activity at 25 μM (maximum concentration assayed). Fluorescence microscopy with the fluorescein–labeled conjugate [Flu]-PEG-[peptide] (compound **4)** demonstrated the low ability of the hydrocarbon-bridged analogues to cross the cell membrane (data not shown). To deliver the peptides into the parasites, **2** was covalently linked to an R_9 sequence used as a CPP (compound **5**), following the successful

strategy already employed for the efficient uptake of the linear peptide prototype **1** and several lactam-bridged and mixed α,β-peptide foldamer analogues [29,33]. The R_9 sequence was also studied in parallel as a control. The EC_{50} values obtained demonstrate that the leishmanicidal activity of **5** against axenic amastigotes and promastigotes is similar to that observed for the reference drugs edelfosine and miltefosine, as well as for the previously obtained linear and lactam cyclic peptide analogues.

Table 4. $EC_{50} \pm SEM$ values for the [R_9]-[stapled peptide] conjugate **5** on *L. infantum* promatigotes, amastigotes and cytotoxic activity in the THP-1 cell line.[a]

Compound[b]	EC_{50} (μM) Promastigotes	EC_{50} (μM) Amastigotes	EC_{50} (μM) THP-1
5 RRRRRRRRRPKPK-$c[(CH_2)_3CH=CH(CH_2)_3]^{3,7}$[A*IQSA*]GISN$_LKN_L$	1.95 ± 0.14	2.14 ± 0.5	0.33 ± 0.05
11 RRRRRRRRR[c]	> 25	> 25	> 25
12 RRRRRRRRR PKIIQSVGISN$_L$KN$_L$[c]	4.6 ± 0.2	3.5 ± 0.9	1.7 ± 0.5
13 RRRRRRRRRPK-$c[(CH_2)_2CONH(CH_2)_4]^{3,7}$[EIQSK]GISN$_LKN_L$[c]	3.5 ± 0.4	2.8 ± 0.3	2.5 ± 0.8
Edelfosine	9 ± 0.2	0.6 ± 0.1	1 ± 0.2
Miltefosine	47.6 ± 0.6	2 ± 0.1	19 ± 1.6

[a]Results are representative of three independent experiments each performed in triplicate. [b]All the peptides are acetylated at the *N*-terminus and contain a carboxamide *C*-terminal group. [c]Data from R_9 conjugates of linear peptide **1** (compound **12**), the corresponding amide-bridged peptide conjugate **13** and the R_9 sequence **11** are taken from reference [29] for comparative purposes.

Conclusions

A series of all-hydrocarbon stapled peptides was designed with the aims of improving the proteolytic stability, enhancing the enzyme inhibition activity and increasing the cell permeability of previously reported linear peptide and lactam-bridged analogues that target the dimerization interface of Li-TryR. Although the new stapled peptides retain potent

inhibitory activity against Li-TryR and are shown to be more resistant to proteolysis, they lose their ability to act as Li-TryR disruptors and appear to act as dimer stabilizers. The structural aspects involved in this unexpected and remarkable reversal in the mode of action await further elucidation. Attempts to co-crystallize Li-TryR with these stapled peptides for X-ray diffraction studies is currently underway as previous attempts of co-crystallization with linear or lactam-bridged analogues were hampered by the finding that the monomeric form of Li-TryR precipitates.

The stapled peptides are not able to cross the cell membrane, as assessed by fluorescence experiments using an FITC-labeled peptide. Nonetheless, conjugation of the most proteolitically stable hydrocarbon-stapled peptide **2** to an R_9 CPP favors intracellular uptake and turns this compound into a molecule highly active against both promastigotic and axenic amastigotic forms of cultured *L. infantum* parasites. Therefore, we conclude that all-hydrocarbon stapling of linear TryR dimerization peptide inhibitors does not significantly enhance cell permeability over that of alternatively cross-linked derivatives but has a major impact on their proteolytic stability as well as on their mode of interaction with the TryR homodimer.

EXPERIMENTAL

1. Chemistry

1.1. General Methods

Unless otherwise noted, analytical grade solvents and commercially available reagents were used without further purification. DIEA, piperidine, Ac$_2$O and EDT were purchased from *Aldrich* (Germany), TFA from Fluka (Germany) and HCTU from Fluorochem (UK). Fmoc-protected amino acids were purchased from Fluorochem (UK), *Polypeptide* (France), *Novabiochem* (Merck, Germany) and *Iris Biotech* (Germany). Fmoc-protected Rink Amide MBHA resin (0.56 mmol/g and 0.38 mmol/g loading) was purchased from *Iris Biotech* (Germany) and *Novabiochem*. All-hydrocarbon stapled peptides **2-5** and linear precursors **8** and **9** were synthesized manually on a 20-position cartridge manifold (*Omega*) in a 20-mL polypropylene syringe (*Dulbecco*) equipped with a porous polyethylene filter. The coupling reactions were carried out on solid phase using microwave radiation in a *Biotage Initiator* reactor in a 5 mL vial. Excluding the coupling reaction on the microwave reactor, the rest of the SPPS reactions were stirred using an *IKA-100* orbital shaker.

After cleavage, the acidic crudes were sedimented in Et$_2$O on a *Hettich Universal* 320R centrifuge at 5000 rpm. All the crude and samples were lyophilized using mixtures water/acetonitrile on a Telstar 6-80 instrument. The monitoring of the reactions was also performed by HPLC/MS through a HPLC-waters 12695 connected to a Waters Micromass ZQ spectrometer. The linear peptides were purified on a *Biotage Isolera* instrument using reverse phase columns (KP-C18-HS 12 g) and the cyclic peptides were purified on a semipreparative HPLC instrument. As the mobile phase, mixtures of A:B were used, where A = 0.05% TFA water and B = acetonitrile with a flow rate of 7 mL/min. The peptides were purified using a gradient from 0% of B to 100% of B in 30-45 min and were detected at 217 nm.

NMR spectra of cyclic peptides **2a, 2b** and **3a** were acquired using a Bruker AV-600 spectrometer, equipped with a cryoprobe, running at 600.13 MHz for ^{1}H. The TOPSPIN software (Bruker Biospin, Karlsruhe, Germany) was used for spectral processing. ^{1}H-chemical shifts (δ), reported in ppm relative to the internal reference sodium 2,2-dimethyl-2-silanpentane-5-sulfonate (DSS), were assigned by the standard sequential method [38], based on the analysis of 2D Homonuclear spectra (^{1}H,^{1}H-COSY, ^{1}H,^{1}H-TOCSY, ^{1}H,^{1}H-NOESY). Once assigned the ^{1}H resonances, 2D ^{1}H,^{13}C-HSQC spectra recorded at natural ^{13}C abundance, were analysed to determine the ^{13}C chemical shifts, which were referenced using the IUPAC recommended ^{1}H/^{13}C ratio (0.25144953 [39]). All the NMR spectra were analysed using the SPARKY software (T.D. Goddard and D. G. Kneller, University of California, USA).

The purity of the peptides was checked by analytical RP-HPLC on an Agilent Infinity instrument equipped with a Diode Array and a C18 Sunfire column (4.6 mm x 150 mm, 3.5 µm). As mobile phase, A:B mixtures were used, where A = 0.05% TFA water and B = acetonitrile. The samples were analyzed at 214 and 254 nm in a gradient from 2% of B to 100% of B in 15 min (gradient 1). HRMS (EI+) was carried out in an Agilent 6520 Accurate-Mass Q-TOF LC/MS spectrometer using water/acetonitrile mixtures. MALDI-TOF mass spectrometer (Voyager DE-STR Applied Biosystems) operated in reflectron mode to obtain better resolution was used for the [R$_9$]-[hydrocarbon-stapled peptide] conjugate **5**.

1.2. Solid-Phase Peptide Synthesis (SPPS)

Peptides were synthesized manually on resin following the standard Fmoc/*t*Bu solid-phase orthogonal protection strategy.

General coupling procedure. Fmoc-protected Rink Amide MBHA resin was swollen in DCM/DMF/DCM/DMF (4 x 0.5 min). Then, the resin was treated with a mixture of DBU:piperidine:DMF (1:1:48, in volume) at room temperature (1 x 1 min) and (3 x 10 min)

and washed with DMF/DCM/DMF/DCM (4 x 0.5 min). Later, to the free $N\alpha$-terminal swollen resin (1 equiv.), a solution of the corresponding Fmoc-AA-OH (1.2 equiv.), HCTU (1.2 equiv.) and DIEA (2.4 equiv.) in dry DMF (5 mL) was added. After sealing the vial, the reaction was heated in a microwave vial equipped with a magnetic stirrer for 10 minutes at 40 ºC. Then, the vial was opened, the supernatant removed and new coupling mixture added. This process was repeated 3 times in total (3 x 10 min) until complete coupling. Finally, the resin was transferred to a fritted syringe, drained and washed extensively (DMF/DCM/DMF/DCM, 5 x 0.5 min). This protocol was repeated for the sequential anchoring of each amino acid. Coupling reactions to primary amines were monitored by the Kaiser ninhydrin test and to secondary amines by the Choranil test. In some cases, the progress of the reactions was also followed by analysis of a small sample of peptidylresin after acidic cleavage in an HPLC-MS instrument.

General acetylation procedure. After elongation of the peptides, the *N*-terminal group was acetylated in all the cases by DBU deprotection of the Fmoc-resin-bounded derivative as mentioned above followed by treatment of the deprotected resin with a mixture of Ac_2O:DIEA:DMF (1:1:1, in volume) at room temperature (1 x 1 min) and (4 x 10 min). The resin was finally washed with DMF/DCM/DMF/DCM (4 x 0.5 min).

Ring closing metathesis (RCM) reaction. To the peptidylresins swollen in anhydrous CH_2Cl_2 (5 mL) in a microwave vial (5–10 mL) second generation Grubb's catalyst (0.2 equiv.) was added and the vial was sealed and gently bubbled with argon. Then, the reaction was heated at 75 ºC using microwave radiation for 1 h. The resin was then filtered and washed successively with CH_2Cl_2/MeOH. Residual ruthenium impurities were removed by stirring the resin bound peptide with a solution of DMSO (50 equiv. relative to the catalyst) in DMF for 12 h. Finally, the resin was washed with DMF/CH_2Cl_2/MeOH (3 x 0.5 min).

General cleavage procedure. The well dried resin-bound derivative (1 volume) in a fritted syringe was treated with TFA:TIPS:H_2O 95:2.5:2.5 (5 volumes) for 4 h at room temperature.

The filtrates were precipitated over cold Et_2O and centrifuged three times at 5000 rpm for 10 min. After removing the supernatant, the pellet was redissolved in water/acetonitrile and lyophilized. The crudes were purified to give the target peptides **2-5** in high purity.

Ac-PK-c[(CH₂)₃CH=CH(CH₂)₃]³,⁷[A*IQSA*]GISNₗKNₗ-NH₂ (2a,b). After elongation of the peptide starting from 0.03 mmol of Rink amide resin, the metathesis reaction was carried out for 1 h following the general protocol under microwave conditions. Then, the cyclic peptide was *N*-acetylated and cleaved from the resin. The crude was purified by reverse phase chromatography using semipreparative HPLC to give the cyclic peptide **2a** as major isomer (11.36 mg, 4% overall yield) and **2b** as minor isomer (3.51 mg, 1% overall yield).

Major isomer **2a**: HPLC (gradient 1): 7.47 min (96% analytical purity). HRMS (ESI,+) m/z: calculated for $C_{70}H_{123}N_{17}O_{17}$ 1473.9283; found 1473.9262 (-1.41 ppm). ¹H-NMR (600 MHz, D_2O : H_2O, 1 : 9) and ¹³C-NMR (150 MHz, D_2O : H_2O, 1 : 9) in Table S1.

Minor isomer **2b**: HPLC (gradient 1): 6.90 min (96% analytical purity). HRMS (ESI,+) m/z: calculated for $C_{70}H_{123}N_{17}O_{17}$ 1473.9283; found 1473.9302 (1.32 ppm). ¹H-NMR (600 MHz, D_2O : H_2O, 1 : 9) and ¹³C-NMR (150 MHz, D_2O : H_2O, 1 : 9) in Table S2.

Ac-PKI-c[(CH₂)₃CH=CH(CH₂)₃]⁴,⁸[A*QSVA*]ISNₗKNₗ-NH₂ (3a). After elongation of the peptide starting from 0.33 mmol of Rink amide resin, the metathesis reaction was carried out for 60 min following the general protocol under microwave conditions. After *N*-acetylation and cleavage from the resin, the crude was purified by semipreparative HPLC to yield the major isomer (*E*) of cyclic derivative **3a** (10 mg, 2% overall yield) as a white solid.

Major isomer **3a**: HPLC (gradient 1): 8.68 min (96% analytical purity). HRMS (ESI,+) m/z: calculated for $C_{73}H_{129}N_{17}O_{17}$ 1515.9752; found 1515.9722 (-1.99 ppm). ¹H-NMR (600 MHz, D_2O : H_2O, 1 : 9) and ¹³C-NMR (150 MHz, D_2O : H_2O, 1 : 9) in Table S3.

Ac-FITC-PEG-PK-c[(CH₂)₃CH=CH(CH₂)₃]³,⁷[A*IQSA*]GISN_LKN_L-NH₂ *(4)*. After elongation of the peptide starting from 0.152 mmol of Rink amide resin (0.38 mmol/g), the metathesis reaction was carried out for 1 h following the general protocol under microwave conditions. Then, the Fmoc group was removed and the resin was treated with {2-[2-(Fmoc-amino)ethoxy]ethoxy}acetic acid (2 equiv.), HCTU (2 equiv.) as coupling reagent and DIEA (4 equiv.) for 2 h at room temperature. Fmoc group was removed and resin was treated with fluorescein isothiocyanate (FITC) (2 equiv.) and DIEA (3 equiv.) at room temperature overnight. The cleavage was carried out following the general protocol and the crude was purified by reverse phase chromatography using semipreparative HPLC to give the major isomer of cyclic peptide **4** (8.80 mg, 3% overall yield).

Major isomer **4**: HPLC (gradient 1): 9.62 min (99% analytical purity). HRMS (ESI,+) m/z: calculated for $C_{95}H_{143}N_{19}O_{24}S$ 1966.0274; found 1966.0339 (3.3 ppm).

Ac-RRRRRRRRR-PK-c[(CH₂)₃CH=CH(CH₂)₃]³,⁷[A*IQSA*]GISN_LKN_L-NH₂ *(5)*.

The general elongation protocol was followed with 0.152 mmol of resin followed by acetylation and cleavage following the general protocol. After purification of the crude, **5** was isolated as a white lyophilized cotton-like solid (17.52 mg, 4% overall yield). Major isomer **5**: **HPLC**: t_R = 7.52 min (G2-100, 15 min), >99% purity (at 214 nm). **MALDI-TOF-MS** $C_{124}H_{231}N_{53}O_{26}$ 2881.07.

Ac-PKA*IQSA*GISN_LKN_L-NH₂ *(8)*. The general protocol for elongation was followed with 0.038 mmol of resin. After acetylation, cleavage and purification, linear precursor **8** was obtained as a white solid (5.25 mg, 9% overall yield).

HPLC (gradient 1): 10.11 min (>99% analytical purity). HRMS (ESI,+) m/z: calculated for $C_{72}H_{127}N_{17}O_{17}$ 1501.9596; found 1501.9600 (0.31 ppm).

Ac-PKIA*QSVA*ISN$_L$KN$_L$-NH$_2$ (9). Following the general protocol for elongation with 0.038 mmol of resin, and after acetylation, cleavage and purification, linear precursor **9** was obtained as a white solid (2.5 mg, 5% overall yield).

HPLC (gradient 1): 6.08 min (97% analytical purity). HRMS (ESI,+) m/z: calculated for $C_{73}H_{129}N_{17}O_{17}$ 1515.9752; found 1515.9732 (-1.29 ppm).

2. Circular dichroism (CD)

CD spectra were recorded in a Jasco J-815 spectropolarimeter (Tokyo, Japan) equipped with a Peltier PTC-423S system. Stocks of known peptide concentration (ca. 0.5-1 mM) were prepared by weighing the lyophilized material. The spectra was acquired in water/30%TFE solutions. TFE was chosen as cosolvent to increase the low water solubility of the peptides and because it is known that TFE stabilize pre-existing secondary structures in short lineal peptides [34,35]. Similar conditions were used previously to determine the CD spectra of related lactam-bridged peptide analogues [29]. All measurements were carried out in triplicate at 25 °C and the cuvette path lengths were 0.1 cm for far UV region (250–195 nm). After subtracting appropriate reference spectra from the sample spectra, CD data were processed with the adaptative smoothing method of the Jasco SpectraAnalysis software. CD data are given in ellipticity units ([θ], $deg.dmol.cm^2.residue^{-1}$). The percentage of α-helicity for **2a** and **3a** was calculated by the method described by Rohl and Baldwin [36] from the mean-residue ellipticity experimentally observed at 222 nm and the number of amino acids.

3. Protease susceptibility assays

Stock solutions of proteinase K were prepared in tris-buffered saline (TBS buffer) (50 μgmL^{-1}) based on weight to volume). Stock solutions of the linear peptide **1** and hydrocarbon stapled peptides **2a** and **3a** (100 μM) were prepared using 10% DMSO in TBS buffer (pH 7.6, Aldrich). For the proteolysis reaction, the former peptide stock solutions (200 μL) were mixed with TBS (120 μL). Then, proteinase K stock solution (80 μL) was added (final concentration enzyme 10 μgmL^{-1}), the solution mixed, and finally allowed to proceed at room temperature with orbital shaking. Then, the enzymatic reaction was quenched (50 μL) at the desired time point (0, 5, 15, 30, 60, 120, 240 and 360 min for linear peptide **1** and 0, 15, 30, 60, 120, 240 and 360, 480 min and 24 h or 0, 60, 120, 180, 240, 300, 360, 420 and 480 min for hydrocarbon-stapled analogues **2a** or **3a**, respectively) by addition of 1% TFA in water/acetonitrile 1:1 (100 μL). 100 μL of the resulting quenched reaction was injected onto an HPLC and the amount of starting peptide present was quantified by mass integration of the peak at 214 nm. Duplicate or triplicate reactions were run for each time point reported and half-lives were determined by fitting time dependent peptide concentration to an exponential decay using GraphPad Prism.

4. Li-TryR oxidoreductase activity

Oxidoreductase activity was determined according to the method described by Hamilton et al. [40]. Briefly, reactions were carried out at 26 ºC (250 μL) in HEPES buffer pH 8.0 (40 mM) containing EDTA (1 mM), NADPH (150 μM), $NADP^+$ (30 μM), DTNB (25 μM), T[S]$_2$ (1 μM), glycerol (0.02%), DMSO (1.5%) and recombinant Li-TryR (7 nM). This standard reaction was modified by increasing DTNB, NADPH and $NADP^+$ concentrations up to 100 μM, 300 μM and 60 μM, respectively, when comparing the activity of the peptides against Li-TryR and H-GR. For IC$_{50}$ determinations the enzyme was pre-incubated with the peptides (concentrations ranging from 75 μM to 0.29 μM) for 5 min prior to the addition of T[S]$_2$ and

NADPH. Enzyme activity was monitored by the increase in absorbance at 412 nm for 1 h at 26 °C in a VERSAmax microplate reader (Molecular Devices, California, USA). All the assays were conducted in triplicate in at least three independent experiments. Data were analyzed using a non-linear regression model with the Grafit6 software (Erithacus, Horley, Surrey, UK).

5. H-GR oxidoreductase activity

Reactions were carried out at 26 °C (250 μL) in HEPES buffer pH 8.0 (40 mM) containing EDTA 1 mM), NADPH (300 μM), NADP$^+$ (60 μM), DTNB (100 μM), oxidized glutathione (GSSG, 1 μM), glycerol (0.02%), DMSO (1.5%) and recombinant H-GR (7 nM). The enzyme was pre-incubated with the peptides at 75 μM for 5 min prior to the addition of GSSG and NADPH. Enzyme activity was monitored by the increase in absorbance at 412 nm at 26 °C in a VERSAmax microplate reader (Molecular Devices, California, USA). All the assays were conducted in triplicate in three independent experiments.

6. Dimer quantitation assay

The stability of the Li-TryR dimeric form in the presence of stapled peptides **2** and **3** and linear precursors **8** and **9** was evaluated using the novel Enzyme-Linked ImmunoSorbent Assay (ELISA) recently developed in our laboratory [10]. Briefly a dual (HIS/FLAG) tagged Li-TryR (400 nM) was incubated in a dimerization buffer (200 μL 300 mM NaCl, 50 mM Tris pH 8.0) for 16 h at 37 °C with agitation and in a humid atmosphere in the presence of different peptide concentration (10 to 90 μM). Next the plates were washed ten times with TTBS (Tween 0.1%, 2 mM Tris, 138 mM NaCl 138 pH 7.6) and incubated with diluted monoclonal α-HIS HRP conjugated antibody (200 μL, Abcam, Cambridge, UK) in BSA (5%) in TTBS for 1 h at room temperature. The plates were washed once again as previously described and 1,2-phenylenediamine dihydrochloride (OPD) substrate (100 μL, Dako, Glostrup, Denmark)

prepared according to manufacturer's instructions was added. The enzymatic reaction was stopped after 10 min with H_2SO_4 (100 µL, 0.5 M) and the absorbances were measured at 490 nm in a VERSAmax microplate reader (Molecular Devices, California, USA). All the assays were conducted in triplicate in at least three independent experiments. Data were analyzed using a non-linear regression model with the Grafit6 software (Erithacus, Horley, Surrey, UK).

7. Cells and culture conditions.

L. infantum axenic amastigotes were grown in M199 (Invitrogen, Leiden, The Netherlands) medium supplemented with 10% heat inactivated FCS, 1 g/L β-alanine, 100 mg/L L-asparagine, 200 mg/L sacarose, 50 mg/L sodium pyruvate, 320 mg/L malic acid, 40 mg/L fumaric acid, 70 mg/L succinic acid, 200 mg/L α-ketoglutaric acid, 300 mg/L citric acid, 1.1 g/L sodium bicarbonate, 5 g/L MES, 0.4 mg/L hemin, 10 mg/L gentamicine pH 5.4 at 37 ºC. THP-1 cells were grown in RPMI-1640 medium (Gibco, Leiden, The Netherlands) supplemented with 10% heat inactivated FCS, antibiotics, 1 mM HEPES, 2 mM glutamine and 1 mM sodium pyruvate, pH 7.2 at 37 ºC and 5% CO_2.

L. infantum promastigotes (MCAN/ES/ 89/IPZ229/1/89) were grown in RPMI-1640 medium (Sigma–Aldrich, St. Louis, MO, USA) supplemented with 10% heat-inactivated fetal calf serum (FCS), antibiotics, and 25 mm HEPES (pH 7.2) at 26 ºC.

8. Leishmanicidal activity and cytotoxicity assays.

Drug treatment of amastigotes was performed during the logarithmic growth phase at a concentration of 1×10^6 parasites/mL at 37 ºC for 24 h. Drug treatment of promastigotes was performed during the logarithmic growth phase at a concentration of 2×10^6 parasites/mL at 26 ºC for 24 h. Drug treatment of THP-1 cells was performed during the logarithmic growth phase at a concentration of 4×10^5 cells/mL at 37 ºC and 5% CO_2 for 24 h. LC_{50} was evaluated by flow

cytometry by the propidium iodide (PI) exclusion method [41]. After selection of the parasite population based on their forward scatter (FSC) and side scatter (SSC) values, live and dead parasite cells were identified by their permeability to PI. This is a conservative procedure that may underestimate EC_{50} values as parasites that become fragmented as a result of cell death are excluded from the analysis. To minimize the presence of fragmented parasites drug treatment never exceeded 24 hours.

Appendix A. Supplementary data

HPLC, HRMS or MALDI-TOF-MS of linear precursors and all-hydrocarbon stapled analogues, ^{1}H- and ^{13}C-NMR data and NMR spectra of stapled peptides **2a,b** and **3a**, proteolysis stability data and TryR dimerization assay data are included.

Supplementary data related to this article can be found at http:// dx.doi.org/10.1016/j.ejmech.2018.xx.xxx.

REFERENCES

1- www.who.int/mediacentre/factsheets/fs375/en updated April 2017.

2- M.C. Field, D. Horn, A.H. Fairlamb, M.A.J. Ferguson, D.W. Gray, K.D. Read, M. De Rycker, L.S. Torrie, P.G. Wyatt, S. Wyllie, I.H. Gilbert, Anti-trypanosomatid drug discovery: an ongoing challenge and a continuing need, Nature Reviews 15 (2017) 217-231.

3- Joo Hwan No, Visceral leishmaniasis: revisiting current treatments and approaches for future discoveries, Acta Tropica 155 (2016) 113-123.

4- A.S. Nagle, S. Khare, A.B. Kumar, F. Supek, A. Buchynskyy, C.J.N. Mathison, N.K. Chennamaneni, N. Pendem, F.S. Buckner, M.H. Gelb, V. Molteni, Recent developments in drug discovery for Leishmaniasis and Human African Trypanomiasis, Chem. Rev. 114 (2014) 11305-11347.

5- A.H. Fairlamb, P. Blackburn, P. Ulrich, B.T. Chait, A. Cerami, Trypanothione: a novel bis(glutathionyl)spermidine cofactor for glutathione reductase in trypanosomatids, Science 227 (1985) 1485-1487.

6- R.L. Krauth-Siegel, H. Bauer, R.H. Schirmer, Dithiol proteins as guardians of the intracellular redox milieu in parasites: old and new drug targets in trypanosomes and malaria-causing plasmodia, Angew. Chem. Int. Chem. 44 (2005) 690-715.

7- See for example, L.S.C. Bernades, C.L. Zani, I. Carvalho, Trypanosomatidae Diseases: From the Current Therapy to the Efficacious Role of Trypanothione Reductase in Drug Discovery, Curr. Med. Chem. 20 (2013) 2673-2696 and references therein.

8- A.E. Leroux, R.L. Krauth-Siegel, Thiol redox biology of trypanosomatids and potential targets for chemotherapy, Mol. Biochem. Parasitol. 206 (2016), 67-74.

9- A. Ilari, A. Fiorillo, I. Genovese, G. Colotti, An update on structural insights into the enzymes of polyamine-trypanothione pathway: targets for new drugs against leishmaniasis, Fut. Med. Chem. 9 (2017) 61-77.

10- M.A. Toro, P.A. Sánchez-Murcia, D. Moreno, M. Ruiz-Santaquiteria, J.F. Alzate, A. Negri, M.J. Camarasa, F. Gago, S. Velázquez, and A. Jiménez-Ruiz, Probing the dimerization interface of *Leishmania infantum* trypanothione reductase with site-directed mutagenesis and short peptides, ChemBioChem 14 (2013) 1212-1217.

11- For reviews on covalent cyclization approach see for example ref. 11-13: C. J. White, A. K. Yudin, Contemporary strategies for peptide macrocyclization, Nature Chemistry 3 (2011) 509-524.

12- Y.H. Lau, P. de Andrade, Y. Wu, D.R. Spring, Peptide stapling techniques based on different macrocyclisation chemistries, Chem. Soc. Rev. 44 (2015) 91-102.

13- T.A. Hill, N.E. Shepherd, F. Diness, D.P. Fairlie, Constraining cyclic peptides to mimic protein structure motifs, Angew. Chem. Int. Ed. 53 (2014) 13020-13041.

14- See for example ref. 14-16: N.E. Shepherd, H.N. Hoang, V.S. Desai, E. Letoize, P.R. Young, D.P. Fairlie, Modular α-helical mimetics with antiviral activity against respiratory syncytial virus, J. Am. Chem. Soc. 128 (2006) 13284-13289.

15- K.K. Khoo, M.J. Wilson, B.J. Smith, M. Zhang, J. Gulyas, D. Yoshikami, J.E. Rivier, G. Bulaj and R.S. Norton, Lactam-Stabilized Helical Analogues of the Analgesic μ-Conotoxin KIIIA, J. Med. Chem. 54 (2011), 7558-7566.

16- M.I García-Aranda, S. González-López, C.M. Santiveri, N. Gagey-Eilstein, M. Reille-Seroussi, M. Martín-Martínez, N. Inguimbert, M. Vidal, M.T. García-López, M.A. Jiménez, R. González-Muñiz and M.J. Pérez de Vega, Helical peptides from VEGF and Vammin hotspots for modulating the VEGF–VEGFR interaction, Org. Biomol. Chem. 11 (2013) 1896-1905.

17- See for example recent reviews in ref. 17-19: X. Xie, L. Gao, A.Y. Shull, Y. Teng, Stapled peptides: providing the best of both worlds in drug development, Fut. Med. Chem. 8 (2016) 1969-1980.

18- P.M. Cromm, J. Spiegel, T.N. Grossmann, Hydrocarbon stapled peptides as modulators of biological function, ACS Chem. Biol. 10 (2015) 1362-1375.

19- L.D. Walensky and G.H. Bird, Hydrocarbon-stapled peptides: principles, practice and progress, J. Med. Chem. 57 (2014) 6275-6288.

20- See for example the first example of a hydrocarbon-stapled analogue that improved oral bioavailability: G.H. Bird, N. Madani, A.F. Perry, A.M. Princiotto, J.G. Supko, X. He, E. Gavathiotis, J.G. Sodroski, L.D. Walensky, Hydrocarbon double-stapling remedies the proteolytic instability of a lenghty peptide therapeutic, Proc. Natl. Acad. Sci. USA 107 (2010) 14093-14098.

21- See for example recent examples and review: P.M. Cromm, J. Spiegel, P. Küchler, L. Dietrich, J. Kriegesmann, M. Wendt, R.S. Goody, H. Waldmann, T.N. Grossmann, Protease-resistant and cell-permeable double-stapled peptides targeting the Rab8a GTPase, ACS Chem. Biol. 11 (2016) 2375-2382.

22- A.L. Edwards, F. Wachter, M. Lammert, A.J. Huhn, J. Luccarelli, G.H. Bird, L.D. Walensky. Cellular uptake and ultrastructural localization underlie the pro-apoptotic activity of a hydrocarbon-stapled BIM BH3 Peptide, ACS Chem. Biol. 10 (2015) 2149-2157.

23- a) Y.Q. Long, S.X. Huang, Z. Zawahir, Z.L. Xu, H. Li, T.W. Sanchez, Y. Zhi, S. De Houwer, F. Christ, Z. Debyser, N. Neamati. Design of cell-permeable stapled peptides as HIV-1 integrase inhibitors, J. Med. Chem. 56 (2013) 5601-5612; b) H. Zhang, Q. Zhao, S. Bhattacharya, A.A. Waheed, X. Tong, A. Hong, S. Heck, F. Curreli, M. Goger,

D. Cowburn, E.Q. Freed, A.K. Debnath. A cell-penetrating helical peptide as a potential HIV-1 inhibitor, J. Mol. Biol. 378 *(*2008) 565-580.

24- Q. Chu, R.E. Moellering, G.J. Hilinski, Y.-W. Kim, T.N. Grossmann, J.T.-H. Yeh, G.L. Verdine, Towards understanding cell penetration by stapled peptides, Med. Chem. Commun. 6 (2015) 111-119.

25- Y. Tian, Y. Jiang, J.Li, D. Wang, H. Zhao, Z. Li. Effect of stapling architecture on physicochemical properties and cell permeability of stapled α-helical peptides: a comparative study, ChemBioChem 18 (2017) 2087-2093.

26- See for example recent review: Z. Qian, P.G. Dougherty, D. Pei, Targeting intracellular protein-protein interactions with cell-permeable cyclic peptides, Curr. Opin. Chem. Biol. 38 (2017**)** 80-86.

27- L.D. Walensky, A.L. Kung, I. Escher, T.J. Malia, S. Barbuto, R. Wright, G. Wagner, G. L. Verdine, S.J. Korsmeyer, Activation of apoptosis in vivo by a hydrocarbon-stapled BH3 helix, Science 305 (2004**)** 1466-1470.

28- R.E. Moellering, M. Cornejo, T.N. Davis, C. Del Bianci, J.C. Aster, S.C. Blaklow, A.L. Kung, D.G. Gilliland, G.L. Verdine, J.E. Bradner. Direct inhibition of the NOTCH transcription factor complex, Nature 462 (2009**)** 182-188.

29- M. Ruiz-Santaquiteria, P.A. Sánchez-Murcia, M.A. Toro, H. de Lucio, K.J. Gutiérrez, S. de Castro, F.A.C. Carneiro, F. Gago, A. Jiménez-Ruiz, M.J. Camarasa, S. Velázquez, First example of peptides targeting the dimer interface of *Leishmania infantum* trypanothione reductase with potent *in vitro* antileishmanial activity, Eur. J. Med. Chem. 135 (2017**)** 49-59.

30- P.S. Kutchukian, J.S. Yang, G.L. Verdine, E.I. Shakhnovich, All-atom model for stabilization of α-chelical structure in peptides by hydrocarbon staples, J. Am. Chem. Soc. 131 (2009) 4622-4627.

31- See also an excellent review by G.L. Verdine describing this technology: Y. Kim, T. Grossmann, G.L. Verdine, Synthesis of all-hydrocarbon stapled α-helical peptides by ring-closing olefin metathesis, Nat. Protocol. 6 (2011) 761-771.

32- MW-assisted RCM conditions were also required for the synthesis of stapled-peptides in: P.A. Sánchez-Murcia, M. Ruiz-Santaquiteria, M.A. Toro, H. De Lucio, M.A. Jiménez, F. Gago, A. Jiménez-Ruiz, M.J. Camarasa, S. Velázquez, Comparison of hydrocarbon- and lactam- bridged cyclic peptides as dimerization inhibitors of of *Leishmania infantum* trypanothione reductase, RSC Adv. 5 (2015) 55784-55794.

33- H. De Lucio, A. Gamo, M. Ruiz-Santaquiteria, S. De Castro, P.A. Sánchez-Murcia, M.A. Toro, K.J. Gutiérrez, F. Gago, A. Jiménez-Ruiz, M.J. Camarasa, S. Velázquez, Improved proteolytic stability and potent activity against *Leishmania infantum* trypanothione reductase of α/β peptide foldamers conjugated to cell-penetrating peptides, Eur. J. Med. Chem. 140 (2017) 615-623.

34- D. Roccatano, G. Colombo, M. Fioroni, A.E. Mark, Mechanism by which 2,2,2-trifluoroethanol/water mixtures stabilize secondary-structure formation in peptides: A molecular dynamics study, Proc. Natl. Acad. Sci. USA 99 (2002) 12179-12184.

35- a) M. Buck, Trifluoroethanol and colleagues: cosolvents come of age. Recent studies with peptides and proteins, Q. Rev. Biophys. 31 (1998) 297-355; b) C.M. Santiveri, D. Pantoja-Uceda, M. Rico, M.A. Jiménez, beta-hairpin formation in aqueous solution and in the presence of trifluoroethanol: A H-1 and C-13 nuclear magnetic resonance conformational study of designed peptides, Biopolymers 79 (2005), 150-162.

36- C.A. Rohl, R.L. Baldwin, Comparison of NH exchange and circular dichroism as techniques for measuring the parameters of the helix-coil transition in peptides, Biochemistry 36 (1997) 8435-8442.

37- A.Y.L. Sim, C. Verma, How does a hydrocarbon staple affect peptide hydrophobicity?, J. Comput. Chem. 36 (2015) 773-784.

38- K. Wüthrich, M. Billeter, W. Braun, Polypeptide secondary structure determination by nuclear magnetic resonance observation of short proton-proton distances, J. Mol. Biol. 180 (1984) 715-740.

39- J.L. Markley, A. Bax, Y. Arata, C.W. Hilbers, R. Kaptein, B.D. Sykes, P.E. Wright, K. Wüthrich, Recommendations for the presentation of NMR structures of proteins and nucleic acids, Pure & Appl. Chem. 70 (1998) 117-142.

40- C.J. Hamilton, A. Saravanamuthu, I.M. Eggleston, A.H. Fairlamb, Ellman's-reagent-mediated regeneration of trypanothione in situ: substrate-economical microplate and time-dependent inhibition assays for trypanothione reductase, Biochem. J. 369 (2003) 529-537.

41- J.F. Alzate, A. Arias, F. Mollinedo, E. Rico, J. de la Iglesia-Vicente, A. Jiménez-Ruiz, Edelfosine induces an apoptotic process in *Leishmania infantum* that is regulated by the ectopic expression of Bcl-XL and Hrk, Antimicrob. Agents Chemother. 52 (2008) 3779-3782.